Journal of Molecular Liquids 390 (2023) 123121

Contents lists available at ScienceDirect

Journal of Molecular Liquids

journal homepage: www.elsevier.com/locate/molliq

Revealing the binding dynamics between catanionic surfactants and lysozyme: A synergistic computational approach coupled with experimental validation

Ramón Rial [a,b,c,*], Michael González-Durruthy [a,d], Zhen Liu [e], Rui L. Reis [b,c], Juan M. Ruso [a]

[a] Soft Matter and Molecular Biophysics Group, Department of Applied Physics and Institute of Materials (iMATUS), University of Santiago de Compostela, 15782 Santiago de Compostela, Spain
[b] 3B's Research Group, I3Bs - Research Institute on Biomaterials, Biodegradables and Biomimetics, University of Minho, Headquarters of the European Institute of Excellence on Tissue Engineering and Regenerative Medicine, Avepark, Zona Industrial da Gandra, 4805-017 Barco GMR, Portugal
[c] ICVS/3B's - PT Government Associate Laboratory, Braga/Guimarães, Portugal
[d] NanoSafety Group, International Iberian Nanotechnology Laboratory, Braga 4715-330, Portugal
[e] Department of Physics and Engineering, Frostburg State University, Frostburg, MD 21532, United States

A B S T R A C T

The binding mechanisms between a mixture of catanionic surfactants, hexadecyltrimethylammonium bromide (CTAB) and dicloxacillin (Diclox), interacting with the lysozyme protein was investigated by combining computational structure-based and spectrofluorometric approaches. The ezPocket method efficiently predicted lysozyme binding sites, which improved the accuracy of molecular docking simulations for the mixture. The estimated IC_{50} values indicated the potency and effectiveness of both ligands in the lysozyme binding pockets. Dicloxacillin showed stronger binding affinity than CTAB, as evidenced by lower IC_{50} values and higher interaction affinity based on ΔG results. Additionally, CTAB induced conformational changes in the lysozyme binding sites, that decreased the binding affinity of dicloxacillin, and vice versa. The outcomes on the synergistic or antagonistic binding in the catanionic system revealed negative cooperativity based on the obtained negative Hill coefficients. Besides, theoretical 2D-isobolograms illustrated the interaction between the ligands, indicating synergistic and antagonistic effects on the lysozyme binding pockets. Experimental validation unveiled that the presence of the catanionic mixture altered the absorption spectrum of lysozyme, decreasing its hydrophobicity and increasing polarity. The interaction between dicloxacillin and lysozyme resulted in fluorescence quenching and a red shift in the emission wavelength, demonstrating a change towards a more polar environment, while in the case of CTAB, the interaction resulted in shifts in the maximum wavelength and tertiary structure unfolding. These findings support the idea that dicloxacillin is a more potent ligand for lysozyme than CTAB, further unravelling their binding interplay, and laying the groundwork for future investigations aimed at rational drug design for potential biomedical applications.

1. Introduction

Lysozyme, an antimicrobial enzyme naturally produced by animals, holds great significance in numerous key functions, playing a pivotal role in the immune system and finding broad spectrum applications in industrial processes. This enzyme is found in a wide range of organisms, from bacteria to humans, and operates by breaking down bacterial cell walls. Its importance has led to extensive research on its structure, function, and uses. Recent studies have highlighted its potential as a therapeutic agent for various diseases, including cancer, inflammatory disorders, and infections. To exemplify, a recent research study revealed that lysozyme can inhibit the growth and spread of breast cancer cells by inducing apoptosis and suppressing cell proliferation [1]. A different study showed that lysozyme can reduce inflammation and improve wound healing in a mouse model of diabetic foot ulcers [2]. In terms of its industrial applications, lysozyme has shown great potential as a natural preservative in the food industry, avoiding the growth of bacteria that cause spoilage [3]; or as a scaffold for the development of novel biocatalysts with improved catalytic activity [4]. Regarding its protein–ligand interactions and complex formation, it has been previously proven that its combination with drugs of different nature, i.e., beta-blocker, anti-tumour, or penicillin antibiotic drugs; modulated its allosteric properties and produced structural and conformational changes, suggesting non-physiological flexing in large blocks affecting α-helices [5–7].

For its part, dicloxacillin, a derivative of penicillin, has long also been recognized for its potent antibiotic properties from the pharmacological point of view which is commonly employed for combating infections caused by Gram-positive bacteria. However, from an exclusively chemical point of view, and due to its amphiphilic nature, its use

* Corresponding author.
E-mail address: ramon.rial@usc.es (R. Rial).

https://doi.org/10.1016/j.molliq.2023.123121
Received 14 June 2023; Received in revised form 25 August 2023; Accepted 19 September 2023
Available online 19 September 2023
0167-7322/© 2023 The Author(s). Published by Elsevier B.V. This is an open access article under the CC BY-NC license (http://creativecommons.org/licenses/by-nc/4.0/).

has garnered attention for its potential surface-active properties. Within this context, surfactants are compounds that lower the surface tension between two substances, typically a liquid and a solid or a liquid and a gas. Their importance is based on their ability to enhance mixing, emulsify substances, and stabilize interfaces [8]. When combined with excipients, surfactants contribute significantly to enhance drug solubility, stability, and distribution. They assist in solubilizing poorly water-soluble drugs by forming micelles that enhance absorption [9]. Surfactants contribute to formulation stability by preventing clumping and phase separation, although excessive use can lead to instability [10]. Moreover, surfactants aid in wetting solid particles, ensuring uniform drug dispersion in dosage forms like tablets [9]. One such surfactant of interest is cetyltrimethylammonium bromide (CTAB), a versatile compound with multiple applications. It's commonly used in cosmetics and personal care products for its emulsifying and conditioning effects. In the field of molecular biology, CTAB is crucial for DNA extraction, where it helps to separate DNA from proteins and other cellular materials [11]. CTAB also plays a crucial part in material science. It's employed in the synthesis of nanoparticles and nanomaterials, where it acts as a stabilizing agent to prevent particle aggregation [12]. In the realm of chemistry, CTAB serves as a cationic surfactant in various reactions. It can solubilize a wide range of compounds in its micellar structures, aiding in chemical reactions and facilitating the formation of organized assemblies [13]. Its unique properties make it valuable for applications like the synthesis of thin films, templates for nanomaterials, and the preparation of functional materials.

When analysing the interaction of lysozyme with a mixture of surfactants, their interplay has shown to have significant effects on the enzyme's structure, stability, activity and more specifically, on the occurrence of synergistic binding effects. It has been attested that cationic surfactants can induce the aggregation of lysozyme, leading to a decrease in its enzymatic activity (i.e., inhibition). The consequences of synergism in the context of the Gibbs free energy of binding for protein–ligand docking complexes can be significant and can be measured by determining the combination index (CI) [14–17]. Due to the fact that the Gibbs free energy of binding (ΔG) is a measure of the strength of the interaction between the ligand and the receptor, then, when the synergism occurs, the binding affinity of two ligands or drugs interacting at the same biophysical environment of the protein is increased, resulting in a more stable and higher binding affinity than if each ligand were binding independently [17]. On the other hand, non-ionic surfactants have been found to stabilize lysozyme and enhance its activity [18]. Several arguments could support the relevance and the necessity of studying this problem as: i) the issue of improved stability of non-ionic surfactants. Regarding the above, the catanionic addition could significantly enhances the stability of lysozyme. The cited stabilization could help to preserve the enzyme's structure and function under different conditions, such as changes in temperature, pH, or storage duration. ii) Enhanced the enzymatic activity: some studies have revealed that the presence of non-ionic surfactants can significantly enhance the catalytic activity of lysozyme. Because these surfactants act as co-factors or modulators that promote the enzymatic reaction, leading to increased efficiency in lysozyme-mediated processes based on non-covalent interactions. Besides, iii) the potential use to increase the solubility properties of lysozyme. It is well known that lysozyme can have limited solubility under certain conditions, which can affect its stability and functionality. Non-ionic surfactants possess unique properties that can enhance solubility, ensuring its availability for various applications and experiments. Another relevant point is iv) improved bioavailability: because the addition of non-ionic surfactants can enhance the bioavailability of lysozyme in complex biological matrices. This could allow for a better binding interaction and accessibility of lysozyme to study its physiological substrates or endogenous molecules, resulting in improved overall biochemical efficacy. Regarding v) the open problem on the biomedical applications: the lysozyme is widely used in biomedical applications, such as wound healing, antimicrobial therapies, and drug delivery systems. Therefore, a proper stabilization and activity enhancement achieved through non-ionic surfactants could contribute to the development of more efficient and reliable lysozyme-based biomedical applications. Furthermore, vi) formulation optimization and industrial enzyme applications, on this direction non-ionic surfactants offer an opportunity to optimize lysozyme formulations, particularly in pharmaceutical and biotechnological industries.

By identifying surfactants that provide enhanced stabilization and activity, formulation scientists could design lysozyme-based products with improved shelf life, efficacy, and bioavailability. As lysozyme finds applications in various industrial processes, including food production, preservation, and biofuel manufacture, then, the possible use of non-ionic surfactants and the study of the mode of docking interaction with lysozyme can potentially improve the stability and activity of lysozyme in these industrial environments.

The aforementioned arguments demonstrate the significance of studying this particular topic and the potential benefits that can arise from investigating the binding interaction effects of non-ionic surfactants on lysozyme stability and activity from the theoretical and experimental point of view [19]. Consequentially, in the present work, we address the study of the critical interplay between the mixture of catanionic surfactant CTAB plus dicloxacillin and lysozyme through the application of molecular docking simulation coupled with combination index (CI) approach and tailored spectrofluorometric assays. As exposed, the fundamental understanding on the interaction between non-ionic surfactants (i.e., CTAB and dicloxacillin) and lysozyme can provide valuable insights into the mechanisms of enzyme stabilization and enhancement. This knowledge could significantly contribute to our broader understanding of enzyme-surfactant interactions, opening up possibilities for similar approaches in stabilizing and enhancing other enzymes or proteins [20].

2. Materials and methods

2.1. Computational approach

2.1.1. Binding pockets predictions

Herein, ezPocket software was applied as an optimal approach to detect the potential binding cavities of the lysozyme receptor stored from the *RCSB Protein Data Bank* (PDB ID: 1HER). The binding pockets prediction algorithm is based on Delaunay triangulation with weighted points or fast Voronoi tessellation that analyzes the concave surface of the enzyme to identify relevant binding pockets. The algorithms use a grid-based approach to calculate the properties of the enzyme surface, such as hydrophobicity, polarity, and shape. Once the software is run, the detected junction cavities, the XYZ coordinates of the associated cavities center and the cavity volumes are obtained and ranked. In addition, all detected cavities are displayed in a 3D visualization window. Herein, four relevant binding pockets were obtained as volumetric maps for the lysozyme receptor the specific three-dimensional discrete space for setting the docking box simulations [21,22] for the cited pockets were the following: i) *pocket 1* grid box size with dimensions of X = 20 Å, Y = 20 Å, Z = 20 Å and grid box center X = 3.27 Å, Y = 24.19 Å, Z = 27.15 Å, with volume equal to 439.92 Å^3; *pocket 2* grid box size with dimensions of X = 20 Å, Y = 20 Å, Z = 20 Å and grid box center X = 3.02 Å, Y = 23.95 Å, Z = 30.74 Å, with volume equal to 444.72 Å^3; *pocket 3* grid box size with dimensions of X = 20 Å, Y = 20 Å, Z = 20 Å and grid box center X = -10.46 Å, Y = 30.31 Å, Z = 5.96 Å, with volume equal to 258.70 Å^3; and *pocket 4* grid box size with dimensions of X = 20 Å, Y = 20 Å, Z = 20 Å and grid box center X = -4.84 Å, Y = 10.25 Å, Z = 13.44 Å, with volume equal to 356.28 Å^3.

2.1.2. Molecular docking

Molecular docking simulation was performed by using AMDock, which is software specifically designed for the efficient prediction of protein–ligand binding modes and affinities. The method used in

AMDock is based on a combination of a genetic algorithm and a grid-based approach. The initial step involves the preparation of the receptor (i.e., lysozyme) and the ligand structures composing the binary catanionic mixture as dicloxacillin (PubChem CID: 18381; MW: 470.3 g/mol) and hexadecyltrimethylammonium bromide – CTAB (PubChem CID: 5974; MW: 364.4 g/mol).

The crystallographic lysozyme structure is set by removing any unwanted co-crystalized ligand and/or water molecules, and the ligands structures belonging to the mixture were prepared by assigning Gasteiger charges and optimizing geometries. The AMDock algorithm then utilizes a hybrid scoring function that combines different energy force field terms to evaluate the binding affinity of the ligand in different orientations and conformations. To search for the optimal binding mode for the isolated ligands and the binary mixture, AMDock employs a hierarchical docking protocol that starts with a coarse-grained search using an FFT-based method followed by a refinement stage using a Monte Carlo algorithm. The predicted binding modes and affinities are further analyzed and validated using different post-docking analysis tools [23].

2.1.3. Mixture combination index (CI) analysis

The mixture combination index (CI) method was proposed to determine the combined binding interaction between a mixture of catanionic CTAB plus dicloxacillin with every lysozyme binging pocket (from 1 to 4). In the context of this computational study, this approach is supported by the principle that two ligand or drugs present synergistic binding affinity if their combined binding effect is greater than the sum of their individual effects, and antagonistic binding affinity if their combined effect is less than the sum of their individual effects. To determine the CI values, we need to test different theoretical concentrations of each drug alone and in combination and measure the binding effect of the combination in the corresponding lysozyme binding pockets. In this scenario, based on the theoretical docking simulation data, it is possible to calculate the CI for each catanionic ligand combination using the following equation:

$$CI_{(CTAB-Dicloxacillin)} = \frac{C_{CTAB}}{C_{i\_CTAB}} + \frac{C_{Dicloxacilline}}{C_{i\_Dicloxacilline}} + \frac{C_{CTAB}C_{Dicloxacilline}}{C_{i\_CTAB}C_{i\_Dicloxacilline}} \quad (1)$$

where C_{CTAB} and $C_{Dicloxacilline}$ are the theoretical concentrations of CTAB and Dicloxacillin in the catanionic mixture-based combination, respectively, and C_{i_CTAB} and $C_{i\_Dicloxacillin}$ are the theoretical concentrations of CTAB and dicloxacillin that produce the same effect when used individually. The $CI_{(CTAB\text{-}Dicloxacillin)}$ value ranges from <1 to >1, where values < 1 indicate synergistic binding effect, values = 1 indicate additive binding effect, and values > 1 indicate antagonistic binding effect. The resulting plot is called theoretical isobologram, and it allows us to visualize the nature and degree of the ligand interaction under combination conditions as in the presence of mixtures.

2.2. Experimental validation

2.2.1. Reagents

Hexadecyltrimethylammonium bromide (CTAB, 99%, ref. n. H5882), sodium dicloxacillin [3 - (2,6 - dichlorophenyl) – 5 – methyl – 4 - Isoxazolyl penicillin] (ref. n. D9016) and lysozyme from chicken egg white (lyophilized power, protein ≥ 90%, ≥40,000 units/mg, ref. n. L6876) were purchased from Sigma-Aldrich and used without further purification. Samples were freshly prepared for each experiment within 1 h. prior to usage. Solutions were made using triple-distilled and degassed water.

2.2.2. UV–vis absorption spectra

UV–vis absorption spectra were measured using a Cary 100 Bio UV–Vis Spectrophotometer, with a spectral range of 225 – 400 nm. A reference solution of lysozyme in aqueous solution at a concentration of 1 mg/mL, equivalent to 0.07 mM, was used for the UV measurements. To analyse the influence each compound had in the absorbance alone, solutions containing pure dicloxacillin and CTAB were added at increasing concentrations, ranging from 0.083 mM to 0.83 mM, while maintaining the lysozyme concentration constant. Also, mixtures of equal concentrations of both ligands were added to the 0.07 mM solution of the protein. The UV data acquisition was repeated twice for each system to ensure accuracy and minimize the possibility of error or misrepresentation. The replicates showed no significant variation, and the data presented represents the mean value of the two results.

2.2.3. Fluorescence emission spectra

Fluorescence emission spectra were recorded using a Cary Eclipse spectrofluorometer with excitation and emission slits set at 5 nm. The data were acquired at a 0.5 nm interval with an average duration of 0.5 s. The excitation wavelength was maintained at 280 nm and the interaction study was performed over the range of 250–550 nm. Inner filter effects were adjusted to prevent erroneous results during the quenching experiments using the expression $F_{corr} = F_{obs} \times 10^{[(A_{exc}+A_{em})/2]}$, where F_{corr} and F_{obs} represent the observed and corrected fluorescence intensities, respectively, and A_{exc} and A_{em} are the absorptions of the systems at the excitation and emission wavelengths. The data were processed using UV–Vis-IR Spectral Software (FluorTools) [24]. To inspect the fluorescence spectra of the Lysozyme-catanionic compound complexes, a similar procedure was followed as in the UV–vis analysis, first adding each ligand alone and then the catanionic mixture. The measurements were taken at various concentrations, ranging from 0.083 mM to 0.83 mM.

2.2.4. Circular Dichroism (CD)

The Far-UV circular dichroism (CD) spectra were collected using a JASCO-715 automatic recording spectropolarimeter (Japan) equipped with a JASCO PTC-343 Peltier-type thermostated cell holder. Quartz cuvettes with a pathlength of 0.2 cm were used. CD spectra were recorded from 190 to 280 nm for pure protein and ligands solutions. The protein concentration was 1 mg/mL, equivalent to 0.07 mM, and a mixture of dicloxacillin and CTAB was added at increasing concentrations ranged from 0.83 to 4.2 mM for both compounds. The instrument settings comprised a resolution of 1 nm, bandwidth of 1 nm, sensitivity of 50 mdeg, response time of 8 s, accumulation of 3, and scan rate of 50 nm/min. Corresponding absorbance contribution of doubly distilled water was subtracted using the same instrumental parameters. The data were expressed as molar ellipticity, calculated as $[\theta]_\lambda = \theta_\lambda M_r/ncl$, where M_r is the molecular mass of the protein, n is the number of residues, c is the protein concentration, l is the path length of the cell, and θ_λ is the ellipticity at a wavelength λ given by the instrument. The measured CD curves represent a combination of the individual spectra of α-helix, β-sheet, β-turn, and randomly coiled conformations. The secondary structure content was analysed using the Dichroweb program and the CONTIN algorithm.

3. Results and discussion

3.1. Computational characterization

3.1.1. Molecular docking on lysozyme interacting with catanionic surfactants

Overall, binding site prediction tends to be a complex and challenging problem, and different methods and approaches may be appropriate depending on the specific application and target molecule. Herein, computational prediction of relevant binding sites of lysozyme was performed by using ezPocket tool, providing us with a total of four possible pockets distributed over the whole surface of the protein. The ezPocket tool is a widely used software for the prediction of binding sites on protein modeling, based on the principle of identification of concave

cavities that can potentially bind ligands (i.e., CTAB and dicloxacillin) and exclusion of convex ones in the protein structure (i.e., lysozyme) by taking into account the shape and size of the enzyme, Fig. 1.

This result is quite reasonable, since lysozyme is a compact globular protein composed of a single polypeptide chain that folds into a series of secondary structures. In addition to its compact shape, lysozyme is also stabilized by several intramolecular interactions, including hydrogen bonds, van der Waals interactions, and disulfide bonds. These interactions help to maintain the protein's tertiary structure and ensure its stability under a wide range of pH and temperature conditions and allows the protein to interact specifically with its physiological substrates [25] or and efficiently allow the coupling of a wide variety of ligands (i.e., CTAB and dicloxacillin).

The IC_{50} is a measure of the concentration at which a substrate or ligand displays 50% of its maximum inhibitory effect in a given target, and it is commonly used to characterize biochemical process. It is also a significant indicator of potency for a particular agent in pharmacology and is conventionally denoted as a molar concentration. It can be used to evaluate the effectiveness of a ligand (i.e., CTAB and dicloxacillin) in binding to a specific binding pocket (i.e., lysozyme). In order to understand the possible synergies or antagonism response (i.e., ΔG docking affinity) for the evaluated catanionic system, we have estimated the IC_{50} values of the binary mixture formed by CTAB plus dicloxacillin within the previously predicted binding pockets of lysozyme, Fig. 2. In this context, the IC_{50} value represents the theoretical concentration at which CTAB (or dicloxacillin) exerts the half of its maximal interaction response (i.e., ΔG docking affinity). This value is typically in used in Pharmacology or Toxicology to determine the degree or potency of the assessed biochemical response [26–30].

Herein, we theoretically suggest that conformational changes in the lysozyme structure potentially induced by dicloxacillin molecule could significantly reduce the binding affinity of CTAB molecule for the lysozyme. This finding implies that the combination of the mixture as specific inhibitors could have unexpected consequences on the lysozyme modulation. In this context, because of the presence of negative response values for the ΔG binding affinity, it is often desirable to analytically restrict the sigmoidal regression curves ("S"-shaped curve) into a three parameter logistic models (maximum ΔG binding affinity, Hill coefficient, C_i that represents a given concentration value associated with each conformational binding pose in the lysozyme pockets from 1 to 4) which can be used to calculate the IC_{50} value from the logistic dose–response equation:

In the present study, the Hill coefficients were obtained to evaluate the type of interactions of the CTAB and dicloxaxillin in every lysozyme binding pocket and it provided relevant information on the analysis of the obtained dose–response curves. The corresponding values-based on the Hill coefficients were negatives for both ligands in overall lysozyme pockets in order as (#CTAB, #Dicloxacillin): Hill coefficient_pocket 1 (-38.6618, −17.7489), Hill coefficient_pocket 2 (-80.1001, −26.6671), Hill coefficient_pocket 3 (-17.9674, −8.2722), Hill coefficient_pocket 4 (-25.1255, −12.4014).

From the mechanistic point of view, a negative Hill coefficient indicates a negative cooperative binding behavior within the evaluated lysozyme binding sites, indicating that the binding of one molecule (i.e., CTAB or/and dicloxacillin) inhibits or antagonize the binding of other molecules. Otherwise (i.e., negative Hill coefficient), indicates positive cooperative of binding, which occurs when the binding of a given molecule increases by means of synergistic effects on the binding to others. From the thermodynamics point of view, in the current study, clearly, the dicloxacillin molecule shows more binding affinity than the CTAB molecules, based on the more negative values obtained for the affinity ΔG values from the formed complexes in all the lysozyme binding pockets. Besides, this fact is in accordance with the lower IC_{50} values obtained for dicloxacillin compared to CTAB for every pocket, Fig. 2. In this case, is theoretically suggested that the Dicloxacillin molecules can accommodate in a more efficient conformational way that the CTAB molecules in a smaller range of millimolar concentrations to induce the lysozyme inhibition. Furthermore, it is so interesting that,

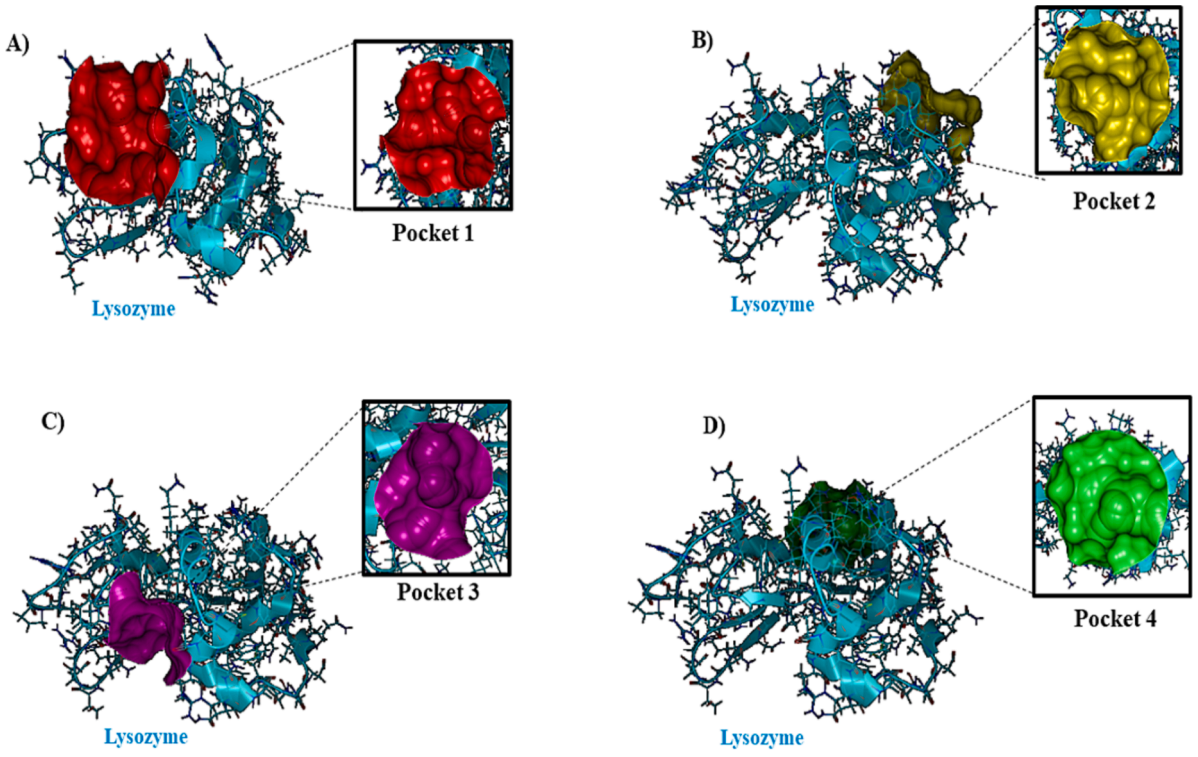

Fig. 1. Representation of the 3D-crystallographic structure of the lysozyme with the associated binding pockets and related position within the whole lysozyme as van der Waals representation. **A)** Binding pocket 1, **B)** binding pocket 2, **C)** binding pocket 3, binding pocket 4. In the right-side of each panel a zoom was performed in order to show the different 3D-crystallographic surface of each binding side.

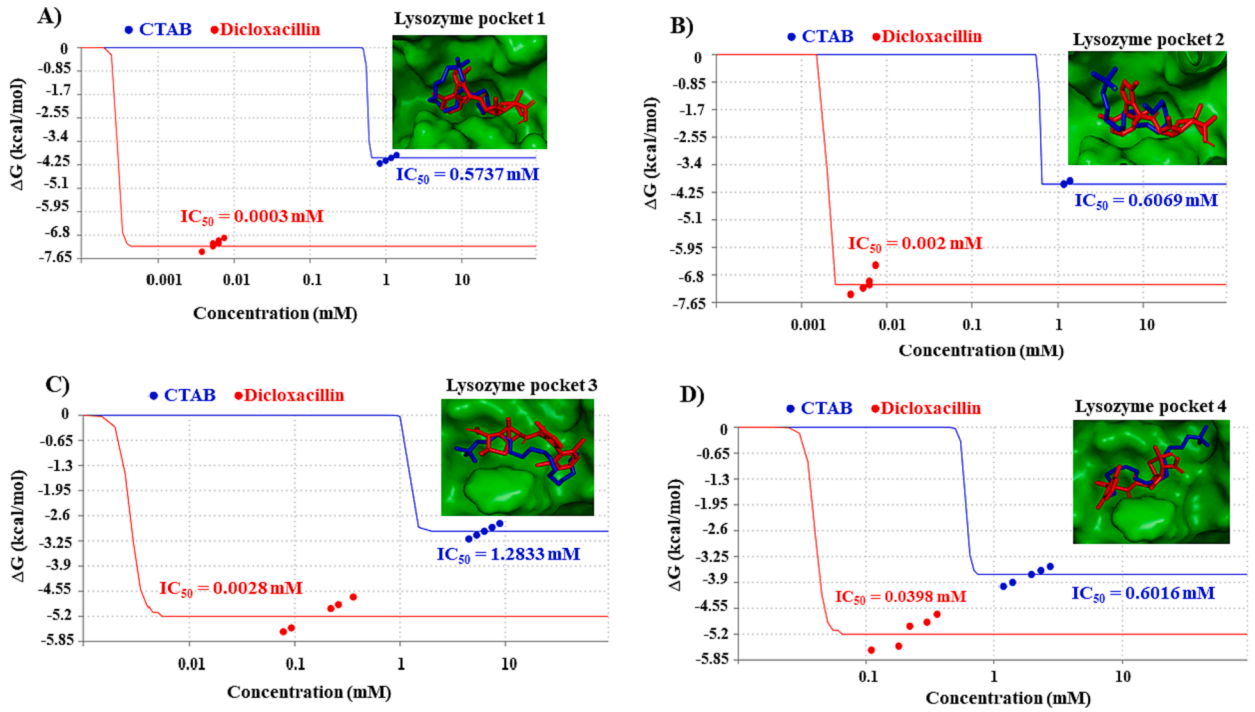

Fig. 2. Graphical results of the sigmoidal shape curves of docking affinity ΔG (kcal/mol) vs. concentrations (mM) obtained from the binding interactions of the catanionic surfactants with the predicted lysozyme binding pockets. Herein, the IC_{50} values were theoretically estimated for each dose–response curves in all the cases by highlighting with color-labels both ligands as CTAB (labelled-blue) and dicloxacillin (labelled-red). In addition, the best crystallographic binding poses as docking complexes were represented in each lysozyme pocket (labelled-green van der Waals regions) as: **A)** CTAB plus dicloxacillin within the pocket 1, **B)** CTAB plus dicloxacillin within the pocket 2, **C)** CTAB plus dicloxacillin within the pocket 3, **D)** CTAB plus dicloxacillin within the pocket 4. Overall results of IC_{50} values and shape of dose–response curves were obtained by using Quest Graph™ IC_{50} calculator.

despite the more negative values of the Hill coefficient for the CTAB molecules compared with the dicloxacillin ones, the binding effect of the dicloxacillin appears to be stronger than CTAB; suggesting the influence of more diversity of docking interactions across the different pockets evaluated, which could contribute to confer more binding stability for the formed docking complex.

Particularly, the binding affinity found under mixture regimen could be strongly influenced by different factors as: i) the evaluated concentration range of the CTAB plus dicloxacillin evaluated, ii) the mixture combination index (CI), and iii) the different amino-acid composition and molecular architecture of the lysozyme pockets. In this regard, it could be plausible the appearance of mechanisms-based on synergistic binding effects simultaneously coexisting with antagonistic binding effects within the same lysozyme pocket. This fact can be properly studied by determining the mentioned combination index (CI) for each lysozyme binding pockets (1 to 4). Specifically, a CI value equal to 1 indicates an additive effect, where the combination of ligands (CTAB and dicloxacillin) produces an effect that is equivalent to the sum of the effects of each drug alone. A CI value of less than 1 indicates synergy, where the combination of drugs produces an effect that is greater than the sum of the effects of each drug alone. On the other hand, a CI value greater than 1 indicates antagonism, where the combination of drugs produces an effect that is less than the sum of the effects of each drug alone. With this aim, the evaluation criterion combination index (CI) in the four simulated conditions by considering the four predictive lysozyme pockets from 1 to 4 was evaluated, (Fig. 3).

In this case, the results of theoretical 2D-isobolograms between CTAB and dicloxacillin correspond to a graphical representation of the interaction between the catanionic surfactant under combination with the lysozyme pockets. The 2D-plots show the concentration ratios of both ligands that produce a specific effect (usually expressed as the fraction affected) when used in combination, against the corresponding concentrations of each ligand that produce the same effect when used alone. The 2D-isobolograms represented above were generated by plotting the theoretical data points on the graph with the x-axis representing the log-concentration of CTAB and the y-axis representing the log-concentration of dicloxacillin.

In this regard, we could strongly suggest the presence of both binding behavior for the mixture of catanionic surfactant interacting with the different binding pockets. As depicted in the Fig. 3, labeled-blue region ($CI_{(CTAB\text{-}Dicloxacillin)} < 1$) corresponds to synergistic binding effects while labeled-red region ($CI_{(CTAB\text{-}Dicloxacillin)} > 1$) corresponds to antagonistic binding effects. Following this idea, a predominance of synergistic binding effects for the lysozyme binding pockets 1, 2 and 4 were identified, with the exception of the pocket 3 where a greater tendency to the appearance of antagonism-based mechanisms with combination indexes $CI_{(CTAB\text{-}Dicloxacillin)} > 1$ were detected for the different log-concentration evaluated. It is important to note that for the lysozyme pocket 4, the relative synergistic binding effect could be attenuated and/or disappear depending on the concentration range of the combinations evaluated for CTAB plus dicloxacillin in the mixture.

This theoretical evidence strongly implies that the architecture of the lysozyme pocket could affect the interactions when analyzing binary or complex mixtures. The definition of synergistic binding effects from the pharmacodynamics point of view, refers to a situation where CTAB plus dicloxacillin work together in a way that their combined or cooperative effect is greater than the sum of their individual effects. This fact means that the binding affinity of CTAB plus dicloxacillin is enhanced, resulting in an overall increase of the docking affinity in certain regions of the lysozyme receptor.

Theoretically, it is possible to find the three different types of synergistic binding effects under the interaction with the mixture of the catanionic surfactant with lysozyme as: i) *additive synergism* when the binding effect of two ligands taken together is equal to the sum of their individual effects: $\Delta G_{(CTAB+Dicloxacillin)} = \Delta G$ [CTAB-Lysozyme] + ΔG [Dicloxacillin-Lysozyme], ii) Potentiative synergism, which occurs

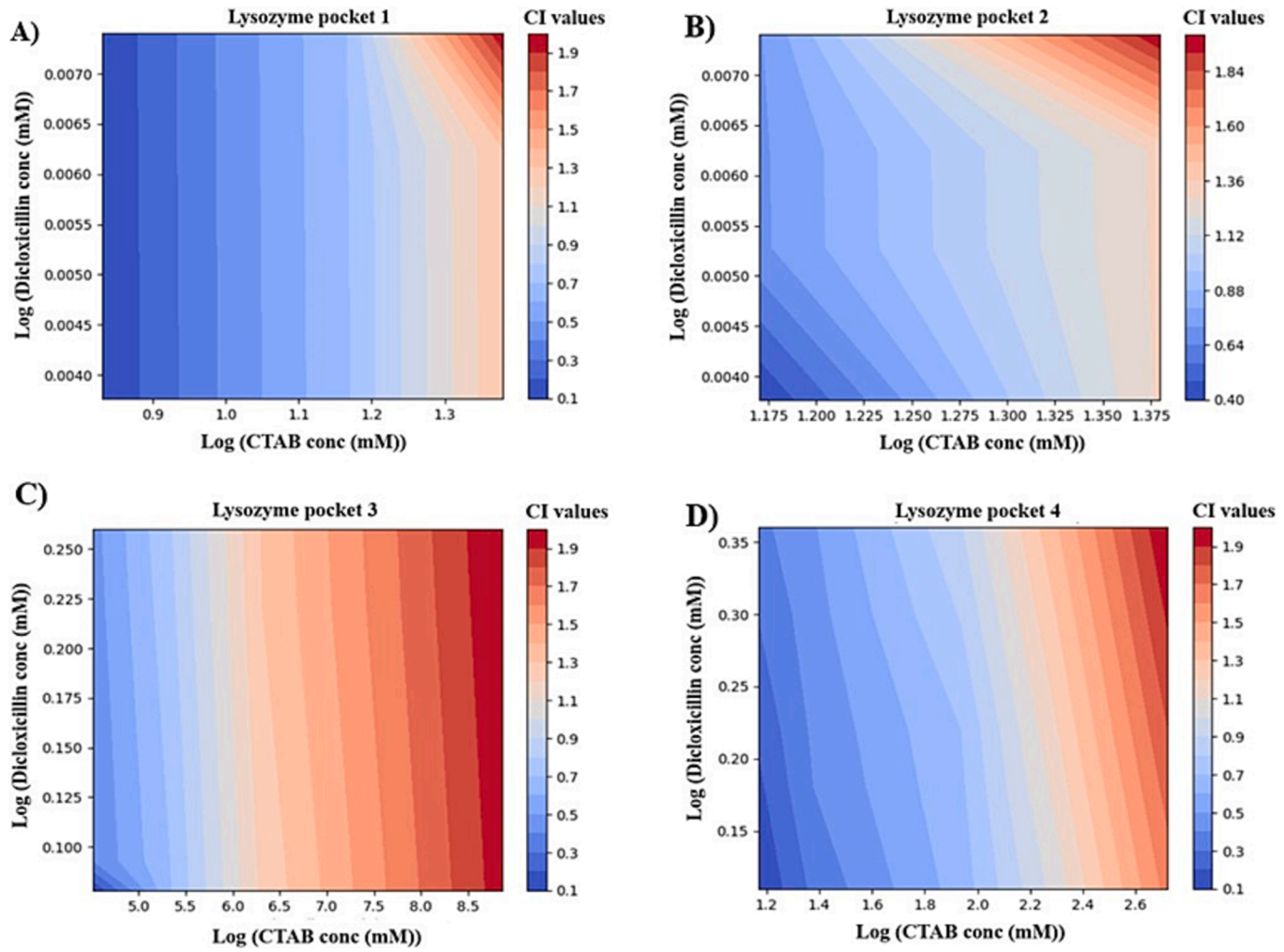

Fig. 3. Graphical representation of the theoretical 2D-isobolograms between CTAB and dicloxacillin under combination for each lysozyme binding pocket (from 1 to 4). Herein, the intensity bar color in the right-side of each isobolograms is to represent the combination index of the binary catanionic mixture as labeled-blue region ($CI_{(CTAB\text{-}Dicloxacillin)} < 1$) corresponds to synergistic binding effects while labeled-red region ($CI_{(CTAB\text{-}Dicloxacillin)} > 1$) corresponds to antagonistic binding effects.

when one ligand or drug (i.e., CTAB) enhances the binding effect of another drug (i.e., Dicloxacillin) as $\Delta G_{(A*B)} = \Delta G$ [CTAB-Lysozyme] * ΔG [Dicloxacillin-Lysozyme], iii) Supra-additive synergism when the binding effect of two ligands taken together (mixture CTAB plus Dicloxacillin) is greater than the sum of their individual effects $\Delta G_{supra} > \Delta G$ [CTAB-Lysozyme] + ΔG [Dicloxacillin-Lysozyme]. To address this point, in the present study, an exhaustive computational exploration of the potential synergistic binding effect of CTAB and dicloxacillin was carried out under interaction with lysozyme.

In the context of protein–ligand interactions, synergism can have several consequences, both positive and negative [31–34]. Positive consequences of synergism in protein–ligand interactions include: i) increased binding affinity based on synergistic interactions between a protein and a ligand can lead to an increase in their affinity for each other, meaning that the ligand binds more tightly to the protein. This can lead to a stronger biological effect or therapeutic benefit. Increased selectivity based on synergistic interactions could lead to potential toxicity, meaning that the ligand binds preferentially to a specific protein over other proteins in the body. This can lead to a more targeted and effective treatment with fewer side effects. ii) Synergistic binding interactions of two compounds with a given allosteric site could affect the resulting global effect by allosteric modulation mainly triggered by the ligand with the best binding affinity. On the other hand, negative consequences of synergism in protein–ligand interactions include: iii) overdosing associated to synergistic interactions can lead to a greater biological effect than expected based on the concentration of the ligand alone. iv) In opposition, antagonistic binding interactions can lead to toxic effects or adverse reactions by competitive binding, where two or more ligands bind to the same site on a protein, reducing the effectiveness of each ligand. This effect could lead to reduced therapeutic benefit or the need for higher doses. Finally, there are the off-target effects based on synergistic interactions, where the ligand binds to unintended proteins, leading to undesired adverse or toxic effects.

In brief, while synergistic interactions between proteins and ligands can have positive consequences such as increased affinity, selectivity, and allosteric modulation, they can also have negative consequences such as overdosing, competitive binding, and off-target effects. Therefore, it is of high importance to understand the potential effects of different ligands. As we can clearly note, the antagonistic binding effects of the mixture of catanionic surfactant points to be more significant for the lysozyme binding pockets 3 followed by the pocket 4 (for certain ranges of CTAB plus dicloxacillin mixture concentration) with an observed predominance of labeled-red region ($CI_{(CTAB\text{-}Dicloxacillin)} > 1$) in the theoretical 2D-isobolograms (Fig. 3, panels **C** and **D**).

3.2. Experimental validation

3.2.1. Spectroscopic analysis

To validate the computational results, a spectroscopic analysis was carried out by examining the spectral curves under different conditions

and concentrations. It can be determined whether a complex is formed and, also, observe any structural changes that may occur due to the formation of new structures [35]. Specifically, lysozyme has two main absorption bands. The stronger one, between 200 and 230 nm, is caused by the π-π* electronic transitions of the peptide backbone C=O and represents the conformation of the lysozyme framework. The weaker band, between 260 and 290 nm, is caused by the absorption of aromatic amino acids and reflects the changes in the chromophore microenvironment [36,37]. The three aromatic amino acids present in lysozyme - tyrosine, phenylalanine, and tryptophan - are the main contributors to this absorption peak. Tryptophan has the strongest contribution among the three and results in a peak at 278 nm. In this particular situation, as both CTAB and dicloxacillin have a maximum absorption peak near that specific wavelength, Fig. 4 **b) and c)**, spectra were corrected making the equivalent subtractions to evaluate the influence the interaction has in the final complex, Fig. 4 **a)**. As detected, the absorption spectrum of lysozyme is affected by the presence of the mixture of both ligands together. At 298 K, and upon complexation with the catanionic complex, the 278 nm band of lysozyme suffers a reduction in its maximum value, suggesting a decrease in hydrophobicity and an increase in polarity [37]. Additionally, another potential cause for the hypochromism could be attributed to the π-π stacking interaction between the phenyl rings of amino acid residues and the aromatic ring present in the dicloxacillin molecule [6], combining hydrophobic forces with charge transfer.

Aside from UV–Vis, fluorescence spectroscopy is one of the most sensitive and trustworthy techniques for examining supramolecular host–guest interactions and to provide further information about the molecular interactions [38]. It uses the change in fluorescence spectra of the guest to evaluate the interaction qualitatively and quantitatively. As shown in Fig. 5 **b)**, the presence of dicloxacillin promotes the quenching of lysozyme fluorescence and the red shift in the highest emission wavelength suggests a change in the Trp and Tyr residues' surroundings, suiting the solvent to a more polar, less hydrophobic, fluorophore environment [39]. Similarly, the addition of CTAB also results in a bathochromic effect on fluorescence, but in this case, the fluorescence intensity increases regularly on interaction. This enhancing fluorescence tendency has been already observed in similar systems involving the use of this surfactant as a ligand agent [40,41]. At a wavelength of 280 nm, both tryptophan and tyrosine residues of the protein can become excited, providing information on global changes in the system [42]. The fluorescence emission of lysozyme without CTAB was highest at a

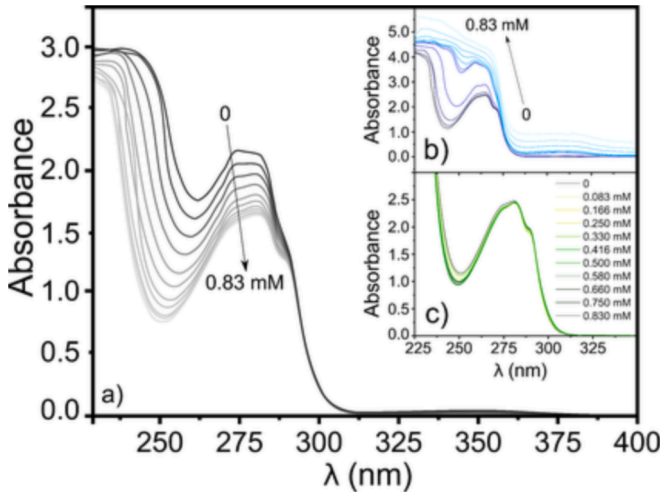

Fig. 4. a) UV absorption spectra of Lysozyme ($C_{lysozyme}$ = 0.07 mM) in the absence and presence of the ligands CTAB/Diclox combined. b) UV absorption spectra of increasing concentrations of Cloxacillin. c) UV absorption spectra of increasing concentrations of CTAB. C_{Diclox} = C_{CTAB} = (0.083, 0.166, 0.250, 0.330, 0.416, 0.500, 0.580, 0.660, 0.750, 0.830) mM.

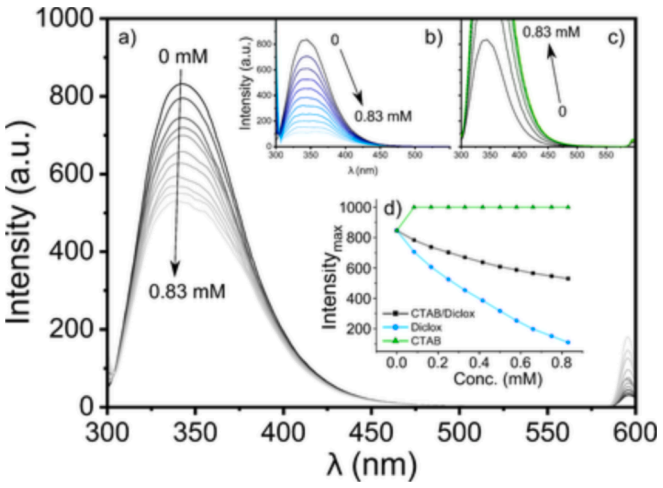

Fig. 5. A) fluorescence emission spectra of lysozyme ($c_{Lysozyme}$ = 0.07 mM) in the absence and presence of the ligands Dicloxacillin and CTAB combined. b) Fluorescence emission spectra of increasing concentrations of Cloxacillin. c) Fluorescence emission spectra of increasing concentrations of CTAB. d) Maximum intensity variation as a function of the concentration of the ligand added. $C_{Dicloxacillin}$ = C_{CTAB} = (0.083, 0.166, 0.250, 0.330, 0.416, 0.500, 0.580, 0.660, 0.750, 0.830 mM.

wavelength of 341 nm after being excited at 280 nm. The change in the maximum wavelength with different concentrations of CTAB was examined, Fig. 5 **c)**. After the addition of CTAB, a meaningful change in both fluorescence intensity and maximum wavelength was observed. As illustrated in the graph, the fluorescence intensity was affected in a dose-dependent manner with a red shift in the maximum wavelength for the different concentrations of CTAB, indicating exposure of fluorophores to the environment. The interaction of CTAB with lysozyme resulted in a high increase in fluorescence intensity, even reaching the saturation of the system, and a shift in maximum wavelength due to the unfolding of the protein tertiary structure caused by weak electrostatic and strong hydrophobic interactions. Similar unfolding behaviour of α-chymotrypsin has also been observed when combined with this surfactant [41]. Lysozyme is positively charged due to the presence of 17 protonated basic residues and 9 deprotonated acidic residues, and CTAB is also positively charged, so only weak electrostatic interactions were evaluated [43].

To gain a better understanding of the molecular interactions occurring in the studied biochemical systems, fluorescence quenching was further inspected. Quenching is the process by which the intensity of a fluorophore's fluorescence decreases due to various chemical interactions with quencher molecules. There are three types of quenching processes that can occur when a fluorophore is paired with a ligand: collisional, static, and mixed processes. Collisional quenching occurs when an excited state fluorophore is neutralized by a quencher through molecular collision. Static quenching involves the formation of a ground state non-fluorescent complexation without relying on diffusion and molecular collision. Finally, mixed quenching is caused by both collision and complex formation with the same quencher. To determine the corresponding mechanism, the Stern-Volmer equation is typically used [44].

$$F_0/F = 1 + K_{sv}[Q] = 1 + k_q\tau_0[Q] \quad (3)$$

where F_0 and F represent the fluorescence intensities in the absence and presence of the quencher, respectively. K_{sv} is the Stern-Volmer quenching constant, which can be used to determine the quenching mechanism. The biomolecular quenching constant, k_q, is a measure of the rate at which the quencher interacts with the fluorophore. The excited state lifetime of the biomolecule in the absence of the quencher, τ_0, is an important parameter for calculating the quenching efficiency.

The value of τ_0 is typically determined experimentally and is dependent on the specific fluorophore being studied. In the case of lysozyme, it is assumed that the value for its excited state lifetime is 5.9×10^{-9} s [45].

Fig. 6 shows a Stern-Volmer plot of F_0/F against [Q]. For purely dynamic (K = 0) or purely static (k = 0) quenching, the plot is linear, while combined quenching (**Eq. (4)** results in an upward curvature [46]. In this case, at higher concentrations the plot deviates significantly from linearity, indicating a coexistence of interactions between lysozyme and dicloxacillin in both the ground and first excited single states, corresponding to static and dynamic quenching, respectively. Thus, considering the product of static and dynamic quenching, the intensity ratio F_0/F can be more accurately described by the equation:

$$F_0/F = (1 + K_S[Q])(1 + K_D[Q]) = 1 + (K_D + K_S)[Q] + (K_D K_S)[Q]^2 \quad (4)$$

The dynamic and static quenching constants are represented by K_S and K_D, respectively. In Fig. 6 **a)**, it can be observed that, at high quencher concentrations, the Stern-Volmer plot shows a continuous ascending curve. A quadratic least square fit was found to be appropriate in this case, with a correlation constant close to 1 ($R^2 = 0.998$). However, at lower concentrations of the drug, $C_{Dicloxacillin} < 5 \cdot C_{Lysozyme}$, the results show a good linear relationship ($R^2 \geq 0.99$). The K_{SV} obtained from the slope at low concentrations and 298 K_{SV} was $(18.36 \pm 0.09) \times 10^3$ L mol^{-1}, and it has been already proved that it decreases with increasing temperature [6]. In case of the mixed ligands, the slope of the plot, is equal to $(7.25 \pm 0.04) \times 10^3$ L mol^{-1}, which corresponds to a quenching constant (k_q) of $(12.88 \pm 0.07) \times 10^{10}$ M^{-1} s^{-1}. By analysing this condition and the measured values of k_q, we can identify the mechanism in the interaction between proteins and ligands. When the interaction is mostly controlled by diffusion, the values of k_q for dynamic quenching are typically in the range of 1×10^{10} M^{-1} s^{-1}. If the values are greater than the diffusion-controlled limit, then the quenching type is static. For CTAB/Dicloxacillin and lysozyme, the quenching rate constant at 25 °C is about 10 times the maximum diffusion rate limit. Therefore, it can be concluded that the interaction is a static quenching process resulting from the formation of a complex.

To determine the binding parameters, such as the number of binding sites (n) and the association constant (k_A), a non-fluorescent complex was assumed to exist between the protein and the ligands. Thus, for the binding interactions, an equilibrium could be presumed, which is described by the following equation:

$$P + nL \rightleftharpoons P - L_n \quad (5)$$

where n is the number of binding sites, P and L are the protein and ligand concentrations. So, the equilibrium constant can be obtained from:

$$k_A = \frac{[P - L_n]}{[P][L]^n} \quad (6)$$

$[P - L_n]$ is the equilibrium concentration. Considering that the complex and drug are non-fluorescent, it can be assumed:

$$[P]_0 = k \times F_0, \quad (7)$$

$$[P] = k \times F \quad (8)$$

$$[L] = [L]_0 - n[P - L_n] \quad (9)$$

$[P]_0$ is the total concentration of protein (0.07 mM) and $[L]_0$ the concentration of the ligands. Then:

$$k_A = \frac{[P]_0 - [P]}{[P]\{[L]_0 - n([P]_0 - [P])} \quad (10)$$

$$\log \frac{[P]_0\text{-}[P]}{[P]} = \log k_A + n \cdot \log \{[L]_0 - n([P]_0 - [P])\} \quad (11)$$

$$\log \frac{F_0\text{-}F}{F} = \log k_A + n \cdot \log \left\{ [L]_0 - n \frac{[P]_0 (F_0 - F)}{F_0} \right\} \quad (12)$$

where F_0 and F are the same as in Eq. (3).

Analysing the experimental data, the average number of binding sites (n) in both systems is close to 1 with the complex lysozyme - dicloxacillin exhibiting a value of 1.49 ± 0.01 while the catanionic complex lysozyme – CTAB/Dicloxacillin resulted in 0.89 ± 0.01 (see Table 1). This suggests the presence of a predominant binding site for dicloxacillin that is "hampered" by the addition of the CTAB as a competitive ligand. These results are in well accordance with the ones obtained theoretically as the computational results obtained from the docking simulations suggest that the affinity of the cationic surfactant mixture on lysozyme follows the order of binding affinity strength as pocket 1 > pocket 2 > pocket 3 > pocket 4. Additionally, the binding affinity of Dicloxacillin, as an inhibitor, was associated with lower values of IC_{50} (half-maximal inhibitory concentration) when interacting with the different lysozyme pockets evaluated, following the same order of binding affinity as pocket 1 > pocket 2 > pocket 3 > pocket 4.

Table 1
Stern-Volmer quenching constants and binding parameters for the interaction of lysozyme with Dicloxacillin and the mixture CTAB/Dicloxacillin at 298 K.

Evaluated systems	Stern-Volmer constants			Binding parameters		
	10^{-2} Ksv (mol^{-1})	10^{-10} kq (mol^{-1} s^{-1})	R^2	n	10^3 K_A (mol^{-1})	R^2
Diclox	18.36 ± 0.09	31.12 ± 0.13	0.997	1.49 ± 0.01	24.45 ± 0.03	0.984
CTAB/Diclox	7.25 ± 0.04	12.88 ± 0.07	0.997	0.89 ± 0.01	0.31 ± 0.02	0.984

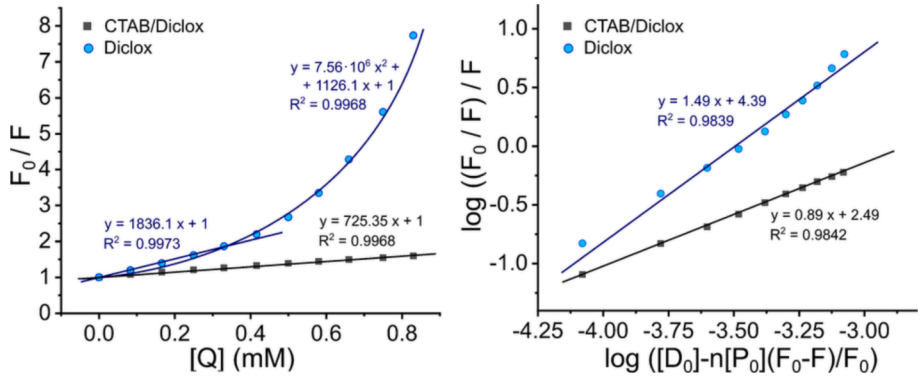

Fig. 6. (a) Stern-Volmer plots for the quenching of Lysozyme by Diclox (○) and CTAB and Diclox combined (■). (b) Plots of log[(F_0-F)/F] vs $log\left\{[D]_0 - n\frac{[P]_0(F_0-F)}{F_0}\right\}$ of Diclox (○) and CTAB and Diclox combined (■). $C_{Lysozyme}$ = 0.07 mM.

Interestingly, the presence of CTAB, seemed to modulate these interactions. The concentration of CTAB at the active site of lysozyme appeared to play a key role in determining whether a synergistic (additive effect) or competitive antagonistic mechanism was observed, depending on the evaluated concentration. Reinforcing the idea that, the interaction between CTAB and dicloxacillin in the lysozyme binding pockets can significantly modulate the negative cooperativity in their binding behaviour.

Furthermore, the binding constant for dicloxacillin is in the order of 10^4 and this value decreases to the order of 10^3 in the mixed system. These binding values strongly suggest that the affinity of the drug towards the biomacromolecule is moderate and once again, the results indicate that CTAB may exhibit a broader range of functions, while dicloxacillin may have a more specific and influential role. Upon analysis of the data, it becomes clear that the potency of dicloxacillin as a ligand for lysozyme significantly surpasses that of CTAB, which is clearly in line with the analysis of the results presented for the IC_{50} value. highlighting its higher potency in inducing lysozyme inhibition.

By the other hand, the energy transfer provided a more comprehensive understanding of the interaction. Fluorescence energy transfer (FRET) has been extensively utilized in researching protein–ligand interactions and changes in protein conformation upon ligand binding. It is a non-destructive spectroscopic approach which can be explained through classical physics, where excitation energy is transferred nonradioactively from the donor molecule (lysozyme) in the excited state to the acceptor molecule(s) in the ground state. Donor molecules usually emit at shorter wavelengths that overlap with the acceptor's absorption spectrum. In the present case, lysozyme fluorescence spectra changes after interacting with ligands reveal that energy transfer occurs between both ligands and the protein. The efficiency of the energy transfer is a good indicator to estimate the distance between the Trp residues in the protein and the ligand [47]. Commonly, the energy transfer occurs when the following requirements are met: (1) the donor emits fluorescent light; (2) the acceptor's UV absorbance spectrum and the donor's fluorescence emission spectrum overlap; and (3) the distance between the donor and the acceptor is less than 7 nm [47]. According to Förster's theory, the efficiency of energy transfer (E) can be calculated using the following expression:

$$E = 1 - (F/F_0) = R_0^6/\left(R_0^6 + r^6\right) \tag{13}$$

F is the fluorescence intensity of lysozyme in presence of ligands while F_0 corresponds to the intensities of the protein alone, r is the binding distance between donor and receptor and R_0 is the critical energy transfer distance, at which 50 % of the excitation energy is transferred to the acceptor. This parameter can be calculated from the following expression:

$$R_0^6 = 8.79 \times 10^{-25} K^2 n^{-4}\, \Phi\, J \tag{14}$$

K^2 denotes the spatial orientation factor between the donor and acceptor dipoles, n represents the refractive index of the medium, Φ is the fluorescence quantum yield of the donor, and J is the spectral overlap between the donor (Lysozyme) emission spectrum and the acceptor (beta-blocker drugs) absorption spectrum. When calculating R_0, the dipole orientation factor is the most imprecise parameter, with a potential range of values from 0 to 4. However, assuming that both the protein and the ligands are rapidly tumbling and can assume any orientation, K^2 is taken as 2/3. The refractive index of water, 1.333, is used for n, and Φ is assumed to be 0.15, corresponding to the fluorescence quantum yield of tryptophan. Finally, the spectral overlap can be determined by:

$$J = \frac{\int_0^\infty F(\lambda)\varepsilon(\lambda)\lambda^4 d\lambda}{\int_0^\infty F(\lambda) d\lambda} \tag{15}$$

F(λ) is the fluorescence intensity of the donor at a given wavelength λ, and ε(λ) is the molar absorption coefficient of the acceptor at wavelength λ.

Accordingly, the overlap curves obtained are presented in Fig. 7. and the corresponding FRET values are listed in Table 2. The catanionic system exhibited a value of the binding distance between donor and receptor, r, within the range of 2–8 nm. Additionally, the conditions of $0.5R_0 < r < 1.5R_0$ strongly suggest that energy transfer from Lysozyme to the ligands is highly probable and supports the presence of non-radiative energy, indicating that the most excited elements could decay to the ground state [44]. Additionally, these findings further reinforce the previously demonstrated fact that the fluorescence mechanisms involved are predominantly of the static type (see Fig. 8).

3.2.2. Circular Dichroism

The far-UV Circular Dichroism is a commonly used method to determine the α-helix and β-sheet secondary structure elements in proteins, which can provide information about their conformational changes [43,48]. In this study, the effect of CTAB and Dicloxacillin on the secondary structure of lysozyme was investigated using far-UV CD spectroscopy. The results showed that upon addition of different concentrations of the mixture CTAB/Dicloxacillin, ranging from 0.83 to 4.2 mM, the shape of the minima significantly changed and the negative ellipticity pointedly decreased, indicating a decrease in the secondary structure of lysozyme [49]. CONTIN algorithm was used to calculate the total percentage of α – Helix structure change, and the results are presented in Table 3.

These findings indicate that the mixture CTAB/Diclox had a notable impact on the secondary structure of the protein. It is worth noting that positively charged surfactants, such as CTAB, can interact with negatively charged residues like Glu and Asp in lysozyme through both weak electrostatic and strong hydrophobic interactions, strengthening the hypothesis presented in the fluorescence analysis. The stabilization effect of CTAB on the secondary structure of lysozyme was mostly attributed to the weak electrostatic interactions, which was confirmed by Gospodarczyk et al. [50]. The decrease in total α-helical content in the presence of CTAB was likely due to the hydrophobic linkage between the hydrophobic chains of CTAB and non-polar residues of lysozyme [51].

4. Conclusions

In the present study the interaction between CTAB and dicloxacillin with lysozyme was addressed by combining structure-based approaches with spectroflorimetric validation to reveal underlying binding mechanisms of the catanionic mixture. The performed ezPocket method efficiently predicted the best-ranked lysozyme binding site (pocket 1), improving the understanding of docking interaction for the CTAB-

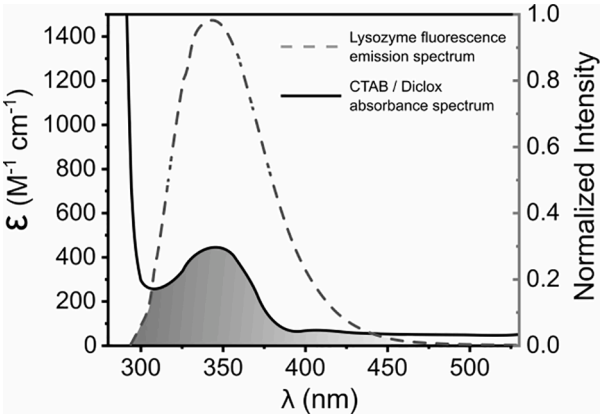

Fig. 7. The overlap of fluorescence emission spectrum (J(λ), grey area) of Lysozyme (dotted line) and absorption spectrum of the mixture CTAB/Diclox (continuous line). $T = 298$ K. $C_{Lysozyme} = 0.07$ mM, $C_{CTAB} = C_{Diclox} = 0.35$ mM.

Table 2
Fluorescence resonance energy transfer (FRET) results of lysozyme with CTAB/Diclox.

Evaluated system	FRET parameters		
	J (M^{-1} cm^{-1} nm^4)	R_0 (Å)	r (nm)
CTAB/Diclox	4.468×10^{12}	17.11	2.05

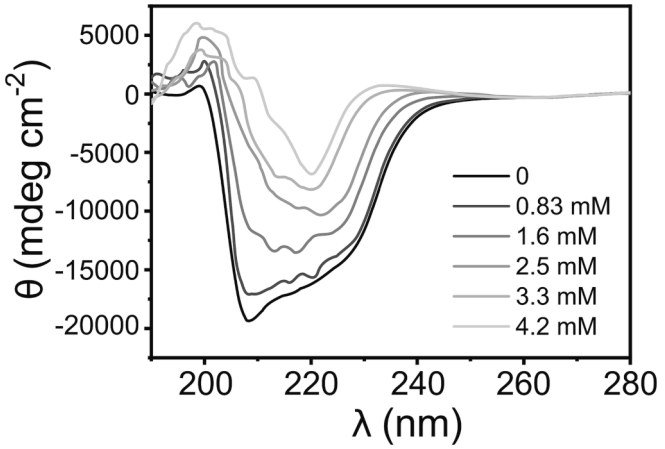

Fig. 8. Far-UV CD spectra of lysozyme without (C_{Lyso} = 0.07 mM, black line) and with increasing concentrations of CTAB/Diclox ($C_{CTAB} = C_{Diclox}$, grey lines).

Table 3
Contents (in %) of the α-helices elements in lysozyme as a function of CTAB/Diclox concentration in (mM).

[CTAB/Diclox] (mM)	α – Helix (%)
0	39.283
0.083	31.741
0.16	22.705
0.25	20.758
0.33	12.398
0.42	11.455

dicloxacillin mixture associated with IC50 values. Regarding the relative potency of catanionic mixture the Dicloxacillin exhibited superior binding affinity that the Cloxacillin showing a more negative ΔG free energy values and lower IC50 scores. Also, CTAB appeared to induce conformational shifts in binding sites, affecting dicloxacillin's affinity.

The study revealed insights into synergistic or antagonistic binding in the catanionic system. CTAB and dicloxacillin's binding in lysozyme pockets indicated negative cooperativity via Hill coefficients. Theoretical 2D-isobolograms highlighted both synergistic and antagonistic effects, with pockets 1, 2, and 4 favoring synergies, while pocket 3 showed antagonism. The presence of catanionic surfactants notably affected lysozyme's absorption spectrum. Complexation lowered hydrophobicity and increased polarity, reducing the 278 nm band linked to π-π stacking. Dicloxacillin caused fluorescence quenching and shifted emission, while CTAB increased intensity and induced protein unfolding. These results reinforced dicloxacillin's superior lysozyme ligand potency, emphasizing its affinity over CTAB. A dominant hindered binding site and energy transfer probability corroborated dicloxacillin's strong affinity.

Lastly, this study significantly advances our understanding of the interplay between mixture of catanionic surfactants with relevant biochemical target as lysozyme, opening new avenues for rational design and potential biomedical applications.

Funding

R.R. and J.M.R. thank Xunta de Galicia for support (ED431B 2022/36), and Ministerio de Ciencia e Innovación (PID2019-805111327GB-100). M.G.D. thanks European Union's H2020 project Sinfonia (N.857253). R.R. is granted by the Program for the requalification, international mobility, and attraction of talent in the Spanish university system, modality Margarita Salas (grant UP2021-042).

CRediT authorship contribution statement

Ramón Rial: Conceptualization, Formal analysis, Methodology, Writing – original draft, Writing – review & editing. **Michael González-Durruthy:** Conceptualization, Software, Methodology, Writing – original draft, Writing – review & editing. **Zhen Liu:** Conceptualization, Writing – review & editing. **Rui L. Reis:** Supervision, Validation. **Juan M. Ruso:** Supervision, Conceptualization, Writing – review & editing.

Declaration of Competing Interest

The authors declare that they have no known competing financial interests or personal relationships that could have appeared to influence the work reported in this paper.

Data availability

Data will be made available on request.

References

[1] L. Jiang, et al., "Recent insights into the prognostic and therapeutic applications of lysozymes," (in Eng), Front. Pharmacol. 12 (2021), 767642.
[2] Q. Chen, W. Li, J. Wang, X. Qu, G. Wang, "Lysozyme-Antimicrobial peptide fusion protein promotes the diabetic wound size reduction in Streptozotocin (STZ)-Induced diabetic Rats," (in Eng), Med. Sci. Monit 24 (2018) 8449–8458.
[3] D.R. Brundige, E.A. Maga, K.C. Klasing, J.D. Murray, Lysozyme transgenic goats' milk influences gastrointestinal morphology in young pigs 1,2, J. Nutrit. 138 (5) (2008) 921–926.
[4] G. Zhang, T. Johnston, M.B. Quin, C. Schmidt-Dannert, Developing a protein scaffolding system for rapid enzyme immobilization and optimization of enzyme functions for Biocatalysis, ACS Synthetic Biol. 8 (8) (2019) 1867–1876.
[5] R. Rial, M. González-Durruthy, M. Somoza, Z. Liu, J.M. Ruso, Unraveling the compositional and molecular features involved in lysozyme-benzothiazole derivative interactions, Molecules 26 (19) (2021).
[6] R. Rial, M. González-Durruthy, Z. Liu, J.M. Ruso, Conformational binding mechanism of lysozyme induced by interactions with penicillin antibiotic drugs, J. Mol. Liquids 358 (2022), 119081.
[7] M. González-Durruthy, R. Rial, Z. Liu, J.M. Ruso, Lysozyme allosteric interactions with β-blocker drugs, J. Mol. Liquids 366 (2022), 120370.
[8] G. Scanavachi, Y.R. Espinosa, J.S. Yoneda, R. Rial, J.M. Ruso, R. Itri, Aggregation features of partially unfolded bovine serum albumin modulated by hydrogenated and fluorinated surfactants: molecular dynamics insights and experimental approaches, J. Colloid Interface Sci. 572 (2020) 9–21.
[9] S.P. Chaudhari, R.P. Dugar, Application of surfactants in solid dispersion technology for improving solubility of poorly water soluble drugs, J. Drug Del Sci. Technol. 41 (2017) 68–77.
[10] D.R. Pokhrel, M.K. Sah, B. Gautam, H.K. Basak, A. Bhattarai, A. Chatterjee, "A recent overview of surfactant-drug interactions and their importance," (in Eng), RSC Adv. 13 (26) (2023) 17685–17704.
[11] J.J. Schenk, L.E. Becklund, S.J. Carey, P.P. Fabre, "What is the "modified" CTAB protocol? Characterizing modifications to the CTAB DNA extraction protocol 11(3) (2023) e11517.
[12] I. Fernando, T. Qian, Y. Zhou, Long term impact of surfactants & polymers on the colloidal stability, aggregation and dissolution of silver nanoparticles, Environ. Res. 179 (2019), 108781.
[13] R. Rial, R.R. Costa, R.L. Reis, Z. Liu, I. Pashkuleva, J.M. Ruso, Mineralization of layer-by-layer ultrathin films containing microfluidic-produced hydroxyapatite nanorods, Cryst. Growth Design 19 (11) (2019) 6351–6359.
[14] L. Huang, Y. Jiang, Y. Chen, Predicting drug combination index and simulating the network-regulation dynamics by mathematical modeling of drug-targeted EGFR-ERK signaling pathway, Scientific Reports 7 (1) (2017) 40752.
[15] Q. Liu, X. Yin, L.R. Languino, D.C. Altieri, Evaluation of drug combination effect using a bliss independence dose-response surface model, Statist. Biopharm. Res. 10 (2) (2018) 112–122.
[16] M. Ezechiáš, T. Cajthaml, Estimation of competitive antagonist affinity by the Schild method and from functional inhibition curves using a novel form of the Gaddum equation, Toxicology 420 (2019) 21–28.

[17] S. Zheng, et al., SynergyFinder Plus: Toward better interpretation and annotation of drug combination screening datasets, Genom. Proteomics Bioinformat. 20 (3) (2022) 587–596.
[18] M.G. Chernysheva, G.A. Badun, A.V. Shnitko, V.I. Petrova, A.L. Ksenofontov, Lysozyme-surfactant adsorption at the aqueous-air and aqueous-organic liquid interfaces as studied by tritium probe, Colloids Surfaces A: Physicochem. Eng. Aspects 537 (2018) 351–360.
[19] P.V. Messina, J.M. Besada-Porto, R. Rial, H. González-Díaz, J.M. Ruso, Computational modeling and experimental facts of mixed self- assembly systems," (in Eng), Cur. Pharm. Des. 22 (34) (2016) 5249–5256.
[20] T. Sharma et al. "Comparative effect of cationic gemini surfactant and its monomeric counterpart on the conformational stability and activity of lysozyme, RSC Adv. 7 27 2017 pp. 16763-16776 10.1039/C7RA00172J.
[21] W.P. Feinstein, M. Brylinski, Calculating an optimal box size for ligand docking and virtual screening against experimental and predicted binding pockets, J. Cheminformat. 7 (1) (2015) 18.
[22] V. Le Guilloux, P. Schmidtke, P. Tuffery, Fpocket: an open source platform for ligand pocket detection, BMC Bioinformatics 10 (1) (2009) 168.
[23] M.S. Valdés-Tresanco, M.E. Valdés-Tresanco, P.A. Valiente, E. Moreno, AMDock: a versatile graphical tool for assisting molecular docking with Autodock Vina and Autodock4, Biology Direct 15 (1) (2020) 12.
[24] S. Preus, DecayFit—Fluorescence Decay Analysis Software 1.3, FluorTools, http://www.fluortools.com, 2014.
[25] H. Schwalbe, et al., Structural and dynamical properties of a denatured protein. Heteronuclear 3D NMR experiments and theoretical simulations of lysozyme in 8 M urea," (in Eng), Biochemistry 36 (29) (1997) 8977–8991.
[26] Y.-C.-M. Hsieh, L. Chang, A.M. Barron, A novel approach for modeling biphasic dose-response curves, Statist. Biopharmaceut. Res. (2023) 1–11.
[27] B.J. Bender, et al., A practical guide to large-scale docking, Nature Protocols 16 (10) (2021.) 4799–4832.
[28] L. Yang J. Wang R.A. Cheke S. Tang A universal delayed difference model fitting dose-response curves 19 4 2021 15593258211062785.
[29] F. Wong, et al., "Benchmarking AlphaFold-enabled molecular docking predictions for antibiotic discovery," (in Eng), Mol Syst Biol 18 (9) (Sep 2022) e11081.
[30] T.T. Nguyen, et al., Robust dose-response curve estimation applied to high content screening data analysis, Source Code Biol. Med. 9 (1) (2014) 27.
[31] S. Zheng, et al., SynergyFinder Plus: toward better interpretation and annotation of drug combination screening datasets," (in Eng), Genom. Proteomics Bioinformat 20 (3) (2022) 587–596.
[32] D.J. Wooten, C.T. Meyer, A.L.R. Lubbock, V. Quaranta, C.F. Lopez, "MuSyC is a consensus framework that unifies multi-drug synergy metrics for combinatorial drug discovery, Nat. Commun. 12 (1) (2021) 4607.
[33] D.J. Wooten, R. Albert, Synergy: a python library for calculating, analyzing and visualizing drug combination synergy, Bioinformatics 37 (10) (2020) 1473–1474.
[34] A. Ianevski, A.K. Giri, T. Aittokallio, SynergyFinder 2.0: visual analytics of multi-drug combination synergies, Nucleic Acids Res. 48 (W1) (2020) W488–W493.
[35] L. Seidel, I. Coin, "Mapping of protein interfaces in live cells using genetically encoded Crosslinkers," (in Eng), MethodsMol Biol 1728 (2018) 221–235.
[36] M. Zaman, et al., Interaction of anticancer drug Pinostrobin with lysozyme: a biophysical and molecular docking approach, J. Biomol. Struct. Dyn. 37 (16) (2019) 4338–4344.
[37] J. Wang et al. Probing the binding interaction between cadmium(ii) chloride and lysozyme, J. Chem. 40 4 (2016) 3738-3746 10.1039/C5NJ02911B.
[38] I. Hussain, S. Fatima, S. Ahmed, M. Tabish, Biophysical and molecular modelling analysis of the binding of β-resorcylic acid with bovine serum albumin, Food Hydrocolloids 135 (2023), 108175.
[39] M. González-Durruthy, R. Rial, M.N.D.S. Cordeiro, Z. Liu, J.M. Ruso, Exploring the conformational binding mechanism of fibrinogen induced by interactions with penicillin β-lactam antibiotic drugs, J. Mol. Liquids 324 (2021), 114667.
[40] J.M. Khan, et al., Effect of Cetyltrimethylammonium bromide (CTAB) on the conformation of a hen egg white lysozyme: a spectroscopic and molecular docking study, Spectrochim. Acta Part A: Mol. Biomol. Spectroscopy 219 (2019) 313–318.
[41] M.S. Celej, M.G. D'Andrea, P.T. Campana, G.D. Fidelio, M.L. Bianconi, "Superactivity and conformational changes on alpha-chymotrypsin upon interfacial binding to cationic micelles," (in Eng), The Biochemist J 378 (Pt 3) (2004) 1059–1066.
[42] T. Janek, Ż. Czyżnikowska, J. Łuczyński, E.J. Gudiña, L.R. Rodrigues, J. Gałęzowska, Physicochemical study of biomolecular interactions between Lysosomotropic surfactants and bovine serum albumin, Colloids Surfaces B: Biointerfaces 159 (2017) 750–758.
[43] I.A. Bhat, W.F. Bhat, M. Akram, D. Kabir ud, Interaction of a novel twin-tailed oxy-diester functionalized surfactant with lysozyme: spectroscopic and computational perspective, Int. J. Biol. Macromol. 109 (2018) 1006–1011.
[44] J.R. Lakowicz, Principles of fluorescence spectroscopy, Springer, 2006.
[45] M.R. Eftink, Fluorescence quenching reactions, in: T.G. Dewey (Ed.), Biophysical and Biochemical Aspects of Fluorescence Spectroscopy, Springer, US, Boston, MA, 1991, pp. 1–41.
[46] P.K. Behera, T. Mukherjee, A.K. Mishra, Simultaneous presence of static and dynamic component in the fluorescence quenching for substituted naphthalene—CCl4 system, J. Luminescence 65 (3) (1995) 131–136.
[47] A.B.T. Ghisaidoobe, S.J. Chung, Intrinsic tryptophan fluorescence in the detection and analysis of proteins: a focus on förster resonance energy transfer techniques, Int. J. Mol. Sci. 15(12), 22518-22538. doi: 10.3390/ijms151222518.
[48] B. Mandal S. Ghosh S.P. Moulik Detailed characterization of lysozyme (Lyz)–surfactant (SDDS) interaction and the structural transitions New J. Chem. 40(5) (2016) 4617–4624 10.1039/C5NJ01498K.
[49] I. Hussain, S. Fatima, S. Ahmed, M. Tabish, Deciphering the biomolecular interaction of β-resorcylic acid with human lysozyme: A biophysical and bioinformatics outlook, J. Mol. Liquids 346 (2022), 117885.
[50] W. Gospodarczyk, M. Kozak, Interaction of two imidazolium Gemini surfactants with two model proteins BSA and HEWL, Colloid Polym. Sc. 293 (10) (2015) 2855–2866.
[51] Y. Wang, R. Guo, J. Xi, Comparative studies of interactions of Hemoglobin with single-chain and with Gemini surfactants, J. Colloid Interface Sci. 331 (2) (2009) 470–475.